Proceedings of the Sixth International Conference on
Railway Technology: Research, Development and Maintenance
Edited by: J. Pombo
Civil-Comp Conferences, Volume 7, Paper 8.2
Civil-Comp Press, Edinburgh, United Kingdom, 2024
ISSN: 2753-3239, doi: 10.4203/ccc.7.8.2

Intelligent and Convenient Detection of Micrometer-Scale Rail Corrugation

X. Tang[1], X. Cai[1], Y. Wang[1], H. Peng[1] and Y. Hou[2]

[1]School of Civil Engineering, Beijing Jiaotong University
China
[2]Department of Civil Engineering, Swansea University
United Kingdom

Abstract

In the process of long-term operation of the railway, rail corrugation seriously affects the safe operation of vehicles and greatly increases the maintenance costs, so it is very necessary to know the degree of rail corrugation in advance. A wavelet packet time-convolutional neural network is proposed to detect micrometer-scale rail corrugation by using car body acceleration, which is a low-cost and fast detection method. By taking the car body acceleration as input, the recognition accuracy of wavelet packet time-convolutional neural network for micron-scale rail corrugation at different wavelengths and amplitudes is compared. The results show that there is strong robustness, superiority of the wavelet packet time-convolutional neural network. The recognition accuracy of the method is 96.60% ~ 99.10% at different wavelengths and 95.40% ~ 100% at different amplitudes, which is a great improvement compared with the traditional model.

Keywords: rail corrugation, wavelet packet decomposition, dilated convolution, residual connection, car body acceleration, vehicle-track coupling dynamics.

1 Introduction

Rail corrugation is a kind of common track disease in high-speed railway [1,2], as shown in Figure 1. Rail corrugation is one of the main causes of increased vibration of the wheel-rail system, which seriously affects the safety of high-speed railway operation and the comfort of passengers [3,4]. It is necessary to carry out regular grinding of the rail corrugation section, and it is especially important to know whether there is rail corrugation accurately before grinding. Therefore, how to accurately and efficiently detect rail corrugation is a crucial subject.

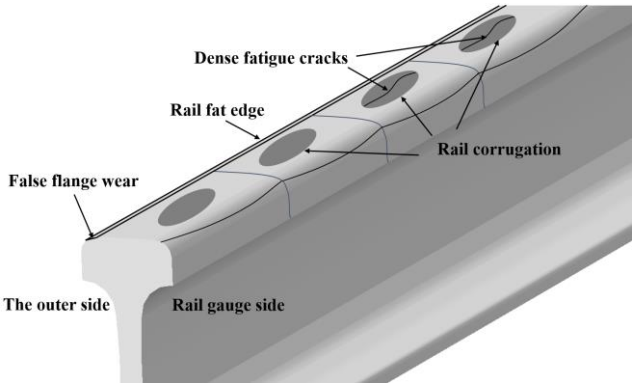

Figure 1: Rail corrugation characteristic diagram.

According to the different principles of rail corrugation detection, it mainly includes the following methods: manual detection method, string measurement method, inertial reference method, machine vision method. The manual detection method requires public works inspectors to use the rail corrugation inspection ruler [5-7] or rail corrugation inspection trolley [6] to measure the rail corrugation on site, which is inefficient and not applicable to the large-scale detection of the rail corrugation. The string measurement method adopts the moving coordinate system based on the rail, due to the measurement of the reference frame of reference with the rail height of the uneven changes in the state of change, resulting in the transfer function (the ratio of the measured value to the actual value) is not constant to 1, resulting in the inevitable error in the measurement of the rail corrugation[7-9]. The inertial reference method characterizes the rail corrugation through the quadratic integration of axle box acceleration, and the wheel state will interfere with the axle box acceleration, so it is impossible to exclude the influence of wheel faults, and due to the use of high-pass filter, the measurement error is relatively large when the vehicle speed is low [10,11]. The machine vision method requires high-precision optoelectronic and camera equipment as well as complex image post-processing techniques, and although the measurement accuracy is high, its application cost is expensive[12-15].

Due to the direct contact between wheels and rails, the appearance of rail

corrugation will cause the vehicle system to produce an obvious dynamic response. Therefore, based on the dynamic response of the vehicle, rail corrugation detection has also been the attention of many experts and scholars. Sunaga et al. [16] proposed that the probability density function of axle box acceleration follows the principle of lognormal distribution. Potter et al. [17] pointed out that the axle box acceleration detection equipment installed in the ordinary operation of the train is relatively easy to operate, the maintenance is also relatively convenient, and at the same time, relatively economic and practical as an auxiliary means of judging the rail corrugation, has great advantages. Hou et al. [18] proposed the use of fuzzy approximation theory can be realized on the prediction of rail corrugation. Roppongi et al. [19] proposed a use of axle box vertical acceleration detection of rail corrugation, gives the range of filtering bands, and realize the positioning of rail corrugation.

Existing studies have mostly used the vibration response of car body components (mostly axle box acceleration) to differentiate between corrugated rail and normal rail. However, the installation location of acceleration sensors on the axle box is limited, and the current installation of axle box acceleration detection train is relatively small, resulting in greater difficulty in acquiring axle box acceleration data. Whereas vibration sensors have more mountable positions in the carriages and are more convenient to install, the data acquisition of car body vibration is relatively easier.

In an effort to address these identified gaps, a wavelet packet time-convolutional neural network (WPTCN) is proposed to detect rail corrugation by using car body acceleration, which is a low-cost and fast detection method. The results of this paper can provide a reference for the detection and assessment of the early stages of rail corrugation, thus helping the public works personnel to scientifically formulate the rail corrugation management programme to ensure the long-term safe operation of high-speed railways.

2 Methods

2.1 Wavelet packet time-convolutional neural network

Based on the vehicle-track coupling dynamics model, the original irregularity is generated according to the German low power spectrum, and the vehicle response is extracted after superimposing different types of micrometer-scale rail corrugation irregularity.

Compared with the German low power spectrum, the amplitude of micron-scale corrugation is smaller, and the frequency band of influence on the vehicle body response is higher. Therefore, the wavelet packet transform is added to the front end of the time convolution neural network to preprocess the input data, and the trend term caused by the German low power spectrum in the vehicle response is eliminated, so that the reconstructed vehicle response can reflect the influence of rail corrugation and better adapt to the recognition effect of the time convolution neural network on the

rail corrugation amplitude. The original vehicle response is input into the WPTCN network, the S1 signal is eliminated, and the S2 ~ S4 signal is reconstructed to form a new signal as input.

WPTCN combines wavelet packet decomposition and reconstruction with time convolution neural network. The Temporal Convolutional Network (TCN) structure consists of two core components: dilated causal convolution and residual blocks. The dilated causal convolution utilizes the dilation factor d ($d=2^l-1$, where l is the dilation rate) to enable the interval sampling of input rail vibration features, as illustrated in Figure 2. In this way, dilated causal convolution enables the use of fewer convolutional layers while achieving a larger receptive field, allowing for capturing more extensive temporal information of the vehicle acceleration.

Each residual block contains two dilated convolution layers, but dilation is only applied once. In the residual block structure, weight normalization can accelerate the network's running speed and enhance the robustness of the network. The spatial dropout factor allows the network to randomly drop neural network units with a certain probability during training to prevent overfitting. The activation function choice of ReLU increases the network's nonlinearity, enhances its expressive power, prevents gradient vanishing, and makes the network sparse. The 1×1 convolutional block allows the network to have the ability to transmit information across layers. The process is shown in Figure 3.

The WPTCN network consists of three different types of residual blocks. The basic structure of each residual block is composed of two convolutional layers, two pooling layers and a residual connection. The size of the convolution kernel in each residual block is 3×1, and the number of convolution kernels is 64. Both pooling layers adopt maximum pooling, with sizes of 4×1 and 2×1, respectively. The expansion coefficients of the three residual blocks are 1, 2 and 4, respectively. The reconstructed vehicle acceleration signal enters the fully connected layer after three residual blocks, and is classified by the softmax function.

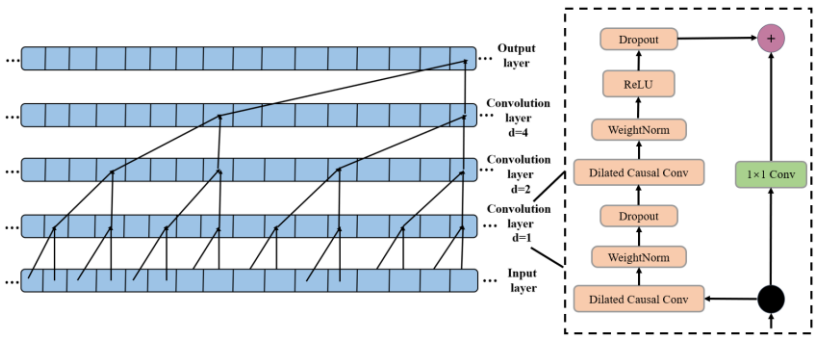

Figure 2: Time convolutional neural network hierarchy diagram.

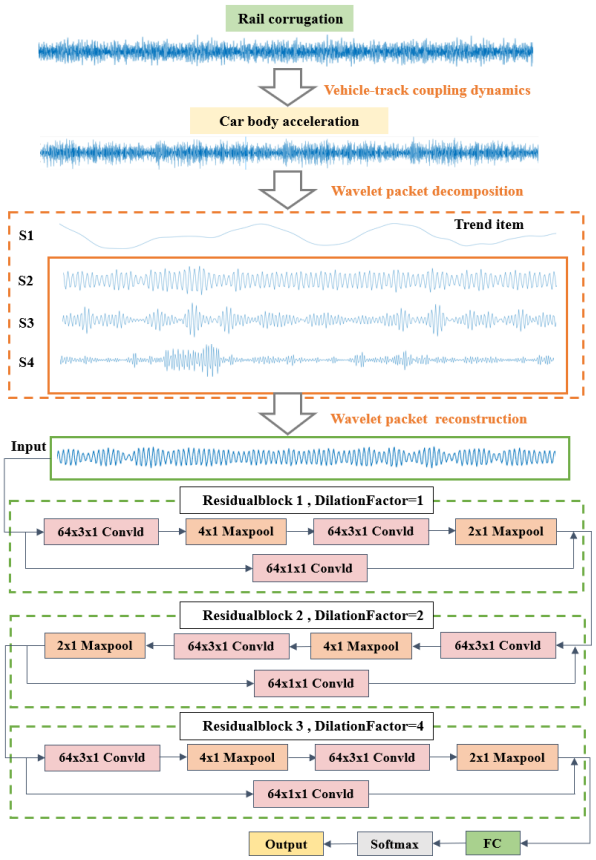

Figure 3: Schematic diagram of micrometer-scale rail corrugation recognition based on WPTCN.

2.2 Vehicle-track dynamic model

The vehicle-track dynamic model developed in this paper makes the following assumptions: each component is regarded as a rigid body, the vehicle model is mainly composed of wheel pairs, bogies and car body, etc. The front and rear bogies have the same structure, and in the bogie model, the front and rear wheel pairs parameters are identical. The elastic deformation of each component is ignored in the model, which is regarded as a multi-rigid body vibration system.

For the vehicle model, the spring damping element is used to simulate the suspension connection between the bogie and the wheelset, the body and the bogie, and the damping force element is used to simulate the transverse and vertical shock absorbers by taking the damping and stiffness in the vertical, transverse and longitudinal directions into consideration as shown in Figure 4. When modeling, the body and bogie are considered to have 5 degrees of freedom and 4 degrees of freedom of the wheelset, with a total of 31 degrees of freedom for the whole vehicle. The detailed parameters of the vehicle are shown in Table 1.

Parameters	Value	Parameters	Value
Car body mass (kg)	3.376×10^4	Longitudinal stiffness of primary spring (N/m)	9.800×10^5
The rolling moment of inertia of the car body (kg·m^2)	1.094×10^5	Lateral stiffness of primary spring (N/m)	9.800×10^5
The nodding moment of inertia of the car body (kg·m^2)	1.655×10^6	Vertical stiffness of primary spring (N/m)	1.176×10^6
The yawing moment of inertia of the car body (kg·m^2)	1.561×10^6	Vertical damping of primary spring (N·s/m)	1.000×10^4
Bogie frame mass (kg)	2.400×10^3	Longitudinal stiffness of secondary spring (N/m)	1.600×10^5
The rolling moment of inertia of the bogie (kg·m^2)	1.944×10^3	Lateral stiffness of secondary spring (N/m)	1.600×10^5
The nodding moment of inertia of the bogie (kg·m^2)	1.314×10^3	Vertical stiffness of secondary spring (N/m)	2.400×10^5
The yawing moment of inertia of the bogie (kg·m^2)	2.400×10^3	Lateral damping of secondary spring (N·s/m)	4.000×10^4
Wheelset mass (kg)	1.850×10^3	Vertical damping of secondary spring (N·s/m)	2.000×10^4
The rolling moment of inertia of the wheelset (kg·m^2)	0.967×10^3	Nominal rolling radius of the wheel (m)	0.43
The nodding moment of inertia of the wheelset (kg·m^2)	0.123×10^3	Distance between the mass centers of the bogies (m)	17.50
The yawing moment of inertia of the wheelset (kg·m^2)	0.967×10^3	Distance of bogie fixed axles (m)	2.50

Table 1: Vehicle parameters.

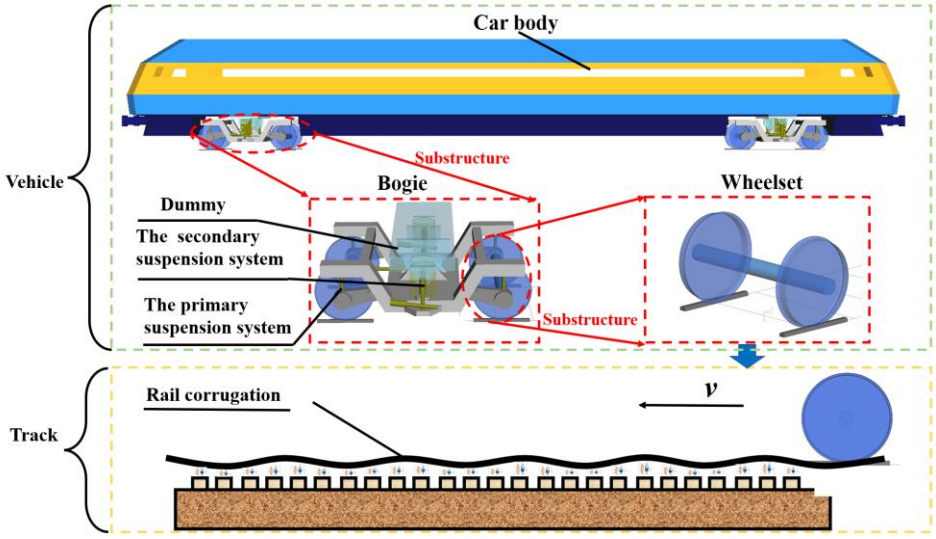

Figure 4: Vehicle-track model.

3 Results

3.1 Robustness of WPTCN

The reconstructed car body acceleration signals under a certain amplitude and wavelength rail corrugation excitation are divided into 200 groups according to the ratio of training set, verification set and test set of 8:1:1, and the robustness of WPTCN is studied.

To comprehensively compare the influence of amplitude and wavelength on the recognition accuracy of WPTCN, the average recognition accuracy of the same amplitude at different wavelengths is calculated firstly. The confusion matrix of the WPTCN is shown in Figure 5. When the amplitude is 0 μm and the wavelengths are 60 mm, 80 mm, 100 mm, 120 mm, 140 mm and 160 mm, the recognition accuracy of WPTCN network is 93.1 %, 100 %, 100 %, 93.1 %, 96.6 % and 100 %, respectively. The average recognition accuracy can be calculated as follows :

(100%×3+93.1%×2+96.6%)/6=97.1%.

According to the above method, the recognition accuracy of WPTCN is calculated, as shown in Figure 6(a). With the change of amplitude, the accuracy does not change regularly. The reason is that in the process of recognition, the WPTCN compares the probability that this type of amplitude is identified as other amplitudes. Under the influence of adjacent amplitudes, the signal change of vehicle body response itself is small. Therefore, the recognition accuracy fluctuates and there is no regularity. However, the recognition accuracy of WPTCN for different amplitudes is more than 95.4 %, and the effect is remarkable.

The average recognition accuracy of the same wavelength at different amplitudes is further calculated. Taking the recognition effect at 60mm wavelength as an example, the recognition rates of 0μm ~ 10μm are 93.1 %, 100 %, 100 %, 96.6 %, 100 %, 100 %, 100 %, 100 %, 100 % and 100 %, respectively. In the case of a wavelength of 60 mm, the average recognition accuracy can be calculated as follows :

(100%×9+96.6%+93.1%)/11=99.1%.

According to the above method, the recognition accuracy of WPTCN is calculated, as shown in Figure 6(b). With the increase of wavelength, the recognition accuracy of WPTCN decreases slightly, which indicates that the increase of wavelength will lead to the decrease of the influence of rail corrugation on the response of the car body, so that the difference between the responses of each car body under different amplitudes is reduced, and the difficulty of WPTCN capturing small fluctuations is increased, which is more difficult to recognize. However, the recognition accuracy of WPTCN for rail corrugation amplitude under different wavelengths is above 96.6 %, indicating that WPTCN has excellent effect on the recognition of micron-scale rail corrugation.

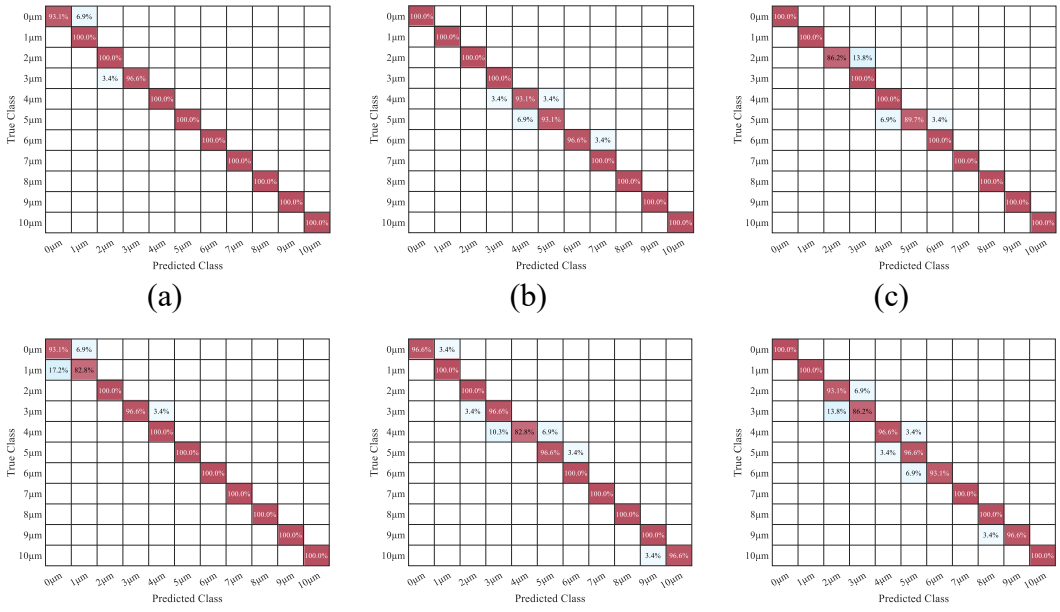

(a) (b) (c)

(d) (e) (f)

Figure 5: The recognition effect of WPTCN on micrometer-scale rail corrugation; (a) 60mm; (b) 80mm; (c)100mm; (d)120mm; (e)140mm; (f)160mm.

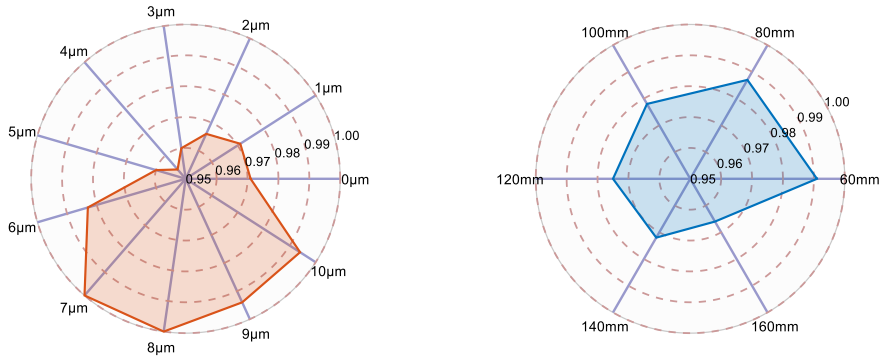

(a) (b)

Figure 6: Robustness of WPTCN; (a) Different amplitudes of rail corrugation; (b) Different wavelengths of rail corrugation.

3.2 Superiority of WPTCN

To further illustrate the superiority of the WPTCN in micrometer-scale rail corrugation recognition, it is compared with Long Short Term (LSTM)[20], Gate Recurrent Unit (GRU)[21], K-Nearest Neighbor (KNN)[22] and Naive Bayesian (NB)[23].

The recognition accuracy of different models for rail corrugation amplitude at different wavelengths is shown in Table 2 and Figure 7. It can be seen that the accuracy

of WPTCN is between 96.6 % and 99.1 %, the accuracy of LSTM is between 55.7 % and 82.9 %, and the accuracy of GRU is between 41.1 % and 72.8 %. The accuracy of KNN is between 13.9 % and 29.8 %, while the accuracy of NB is between 11.9 % and 30.4 %. The KNN and NB models have very low ability to recognize micron-scale rail corrugation. The accuracy of LSTM and GRU models can reach up to 82.9 %, which is significantly better than that of KNN and NB. The recognition accuracy of the WPTCN is up to 99.1%, and that of the traditional model is up to 82.9%. Thus the recognition accuracy of WPTCN is 16.2% higher than the traditional model.

Rail corrugation wavelength value (mm)	WPTCN	LSTM	GRU	KNN	NB
60	99.10%	82.90%	72.80%	29.80%	30.40%
80	98.70%	79.10%	68.40%	28.50%	26.00%
100	97.80%	68.40%	58.90%	21.52%	25.30%
120	97.50%	63.30%	55.70%	19.60%	17.70%
140	97.20%	59.50%	50.60%	16.50%	14.60%
160	96.60%	55.70%	41.10%	13.90%	11.90%

Table 2: Recognition accuracy at different rail corrugation wavelengths.

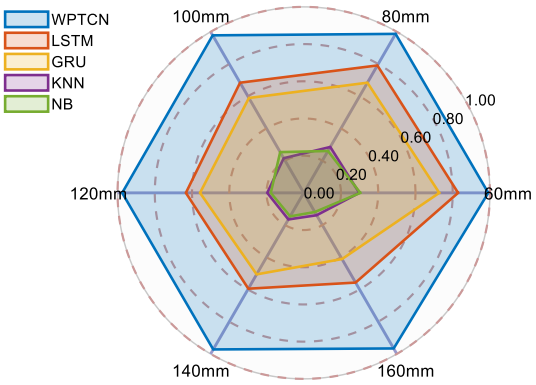

Figure 7: Recognition accuracy at different rail corrugation wavelengths.

On the other hand, the recognition accuracy of different models is affected by wavelength. It can be seen that the accuracy of WPTCN, LSTM, GRU, KNN and NB decreases with the change of wavelength. When the wavelength increases from 60 mm to 160 mm, the accuracy is reduced by 2.5 %, 27.2 %, 31.7 %, 15.9 % and 18.5 %, respectively. The recognition accuracy of KNN and NB is low. Therefore, with the decrease of wavelength, the decrease of recognition accuracy is less than that of LSTM and GRU models. The accuracy of the LSTM and GRU models can be reduced

by up to 31.7 %, which is greatly affected by the wavelength. It shows that the traditional deep learning model is difficult to adapt to the gradual reduction of the car body response caused by the change of wavelength when perceiving the influence of micrometer-scale rail corrugation on the car body response. WPTCN solves this problem well. Whether it is short-wavelength rail corrugation or long-wavelength rail corrugation, its perception of rail corrugation amplitude is at a high level.

To comprehensively compare the recognition capability of different models on the amplitude, the recognition accuracy of different models for a single amplitude is calculated, as shown in Table 3 and Figure 8. When the amplitude is 0μm, the recognition accuracy of the WPTCN can reach 97.1 %, which is 62.4 % higher than that of the other four models. When the amplitude is 1μm, the recognition accuracy of the WPTCN network is 97.1 %, which is 75.7 % higher than that of the other four models. When the amplitude is 2μm, the recognition accuracy of the WPTCN network is 96.6 %, which is 58.8 % higher than the other four models. When the amplitude is 3μm, the recognition accuracy of the WPTCN network is 96.0 %, which is 38.5 % higher than the other four models. It can be seen that the traditional model has a better capability in identifying the rail corrugation with the amplitude is 10μm, but the recognition accuracy is unstable when the amplitude is small. However, the WPTCN can guarantee the recognition accuracy of micrometer-scale rail corrugation when the amplitude is small. Therefore, compared with the traditional model, the WPTCN has greatly improved the recognition accuracy of micrometer-scale rail corrugation.

Rail corrugation amplitude value (μm)	WPTCN	LSTM	GRU	KNN	NB
0	97.10%	33.10%	34.70%	21.70%	22.10%
1	97.10%	21.40%	9.30%	13.60%	25.20%
2	96.60%	37.80%	5.50%	11.50%	5.40%
3	96.00%	57.50%	34.30%	5.60%	4.20%
4	95.40%	73.30%	59.00%	9.20%	3.90%
5	96.00%	89.70%	57.40%	19.40%	17.00%
6	98.30%	83.10%	69.10%	21.70%	20.50%
7	100.00%	99.00%	87.10%	16.90%	24.60%
8	100.00%	100.00%	90.40%	29.50%	28.20%
9	99.40%	90.20%	93.70%	6.00%	13.40%
10	99.40%	100.00%	96.90%	97.60%	86.30%

Table 3: Recognition accuracy at different rail corrugation amplitudes.

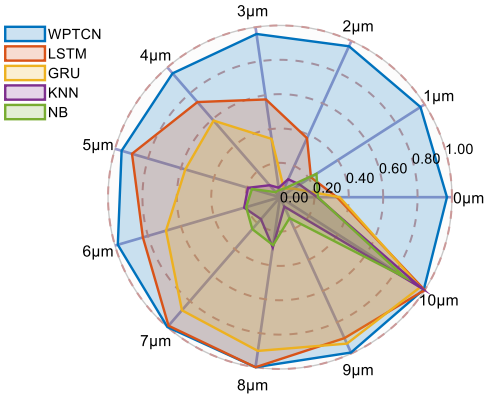

Figure 8: Recognition accuracy at different rail corrugation amplitudes

4 Conclusions and Contributions

In this study, a wavelet packet time-convolutional neural network (WPTCN) is proposed to detect micrometer-scale rail corrugation by using car body acceleration, which is a low-cost and fast detection method, and the robustness, superiority of WPTCN are demonstrated.

The car body acceleration is decomposed by wavelet packet.The S1 component mainly represents the influence of the German low interference spectrum on the car body acceleration, and the high-frequency vibration of the rail corrugation on the car body acceleration has a large influence, which is mainly embodied in S2~S4. Therefore, S2~S4 are utilised to reconstruct the car body acceleration as an input to the WPTCN.

The WPTCN has a high recognition accuracy for micron-scale rail corrugation abrasion of different wavelengths and amplitudes, which indicates good robustness. The recognition accuracy of WPTCN is 96.60% ~ 99.10% at different wavelengths and 95.40% ~ 100% at different amplitudes, which is a great improvement compared with the traditional model, which indicates its superiority.

The contributions of this paper can provide a reference for the detection and assessment of the early stages of rail corrugation, thus helping the public works personnel to scientifically formulate the rail corrugation management programme to ensure the long-term safe operation of high-speed railways.

Acknowledgments

The work was supported by the National Key R&D Program of China (No. 2022YFB2602901), the Project of Science and Technology Research and

Development Program of China State Railway Group Co.. Ltd. (No. SY2022T002) and the National Natural Science Foundation of China (No. 52178405).

References

[1] X. Cai, X. Tang, W. Chang, et al., “Machine learning-based rail corrugation recognition: a metro vehicle response and noise perspective”, Philosophical Transactions of the Royal Society A, 381, 20220171, 2023. (https://doi.org/10.1098/rsta.2022.0171)

[2] X. Tang, Z. Chen, X. Cai, et al., “Ballastless track arching recognition based on one-dimensional residual convolutional neural network and vehicle response”, Construction and Building Materials, 408, 13362, 2023. (https://doi.org/10.1016/j.conbuildmat.2023.133624)

[3] X. Tang, X. Cai, H. Peng, et al., “Experimental and simulation investigation into the cause and treatment of rail corrugation for metro”, Journal of Central South University, 29, 3925−3938, 2022. (https://doi.org/10.1007/s11771-022-5179-2)

[4] X. Cai, X. Tang, S. Pan, et al., “Intelligent recognition of defects in high-speed railway slab track with limited dataset”, Computer-Aided Civil and Infrastructure Engineering, 1-18, 2023. (https://doi.org/10.1111/mice.13109)

[5] S. Wang, Y. Xu, Y. Zhou, et al., “Detection and evaluation of curve corrugation of urban mass transit”, Urban Mass Transit, 10, 56-60, 2011. (https://doi.org/10.16037/j.1007-869x.2011.10.021)

[6] S. Grassie, “Rail corrugation: advances in measurement, understanding and treatment”, Wear, 258, 1224-1234, 2005. (https://doi.org/10.1016/j.wear.2004.03.066)

[7] L. Luo, G. Zhang, W. Wu, et al., “Control of track smoothness in wheel-track systems”, Beijing: China Railway Press, 115-135, 2006.

[8] L. Chen, “Research on key issue of rail corrugation dynamic measurement based on chord measurement method”, Hunan University, 2019. (https://doi.org/10.227135/d.cnki.ghudu.2019.002497)

[9] H. Wei, H. Liu, Z. Ma, et al., “A wide-area measurement method of rail corrugation based on the combination-chord system”, Journal of Northwest University (Natural Science Edition), 48, 199-208, 2018. (https://doi.org/10.16152/j.cnki.xdxbzr.2018-02-007)

[10] S. Grassie, “Measurement of railhead longitudinal profiles: a comparison of different techniques”, Wear, 191, 245−251, 1996. (https://doi.org/10.1016/0043-1648(95)06732-9)

[11] J. Xu, P. Wang, L. Wang, et al., “Research on the distribution characteristics and influence factors of sensitive wavelength of track vertical profile irregularity”, Journal of the China Railway Society, 37, 72-78, 2015.

(https://doi.org/10.3969/j.issn.1001-8361.2015.07.012)
[12] F. Zhou, G. Zhang, K. Zhu, et al., “Laser vision dynamic measuring device and measuring method for rail wear”, 200510123725. 0, 05-24, 2006.
[13] W. Wang, Q. Liu, H. Wang, et al., Laser measuring equipment for rail corrugation. 201220116237. 2, 11-07, 2012.
[14] Q. Li, H. Zhang, S. Ren, et al., “Detection method for rail corrugation based on rail image feature in frequency domain”, China Railway Science, 37, 24-30, 2016. (https://doi.org/10.3969/j.issn.1001-4632.2016.01.04)
[15] Z. Ma, Y. Dong, H. Liu, et al., “Rail corrugation dynamic measurement method based on multi-line structured-light vision”, Chinese Journal of Scientific Instrument, 39, 189-197, 2018. (https://doi.org/10.19650/j.cnki.cjsi.J1803154)
[16] Y. Sunaga, T. Ide, M. Kanao, “A Practical use of axle-box acceleration to control the short wave track irregularities on Shinkansen”. Quarterly Report of RTRI, 9, 35-40, 1995.
[17] R. Potter, G. Kopp, H. Green, “Visible speech”, New York: Van Nostrand, 1947.
[18] B. Hou, Z Xu, P. Gong, “Prediction of damage to in-service steel rails”, Journal of the China Railway Society, 20, 127-131, 1998.(https://doi.org/10.3321/j.issn:1001-8360.1998.03.023)
[19] M. Roppongi, Y. Shibuya, K. Chiyoda, “A new detecting method for rail corrugation by using wavelet analysis”, World Congress of Rail Research, 919 1999.
[20] A. Tanhadoust, T. Yang, F. Dabbaghi, et al., “Predicting stress-strain behavior of normal weight and lightweight aggregate concrete exposed to high temperature using LSTM recurrent neural network”, Construction and Building Materials, 362, 127903, 2023. (https://doi.org/ 10.1016/j.conbuildmat.2022.129703)
[21] Q. Yuan, J. Wang, M. Zheng, et al., “Hybrid 1D-CNN and attention-based Bi-GRU neural networks for predicting moisture content of sand gravel using NIR spectroscopy”, Construction and Building Materials, 350, 128799, 2022. (https://doi.org/10.1016/j.conbuildmat.2022.128799)
[22] L. Viale, P. Alessandro, F. Alessandro, et al., “Least squares smoothed k-nearest neighbors online prediction of the remaining useful life of a NASA turbofan”, Mechanical Systems and Signal Processing, 190, 110154, 2023. (https://doi.org/10.1016/j.ymssp.2023.110154)
[23] H. Nguyen, J. Lafave, Y. Lee, et al., “Rapid seismic damage-state assessment of steel moment frames using machine learning”, Engineering Structures, 252, 113737, 2022. (https://doi.org/10.1016/j.engstruct.2021.113737)